

# International Conference on Space Optics—ICSO 2018

Chania, Greece

9–12 October 2018

*Edited by Zoran Sodnik, Nikos Karafolas, and Bruno Cugny*



## *ATLID, ESA atmospheric LIDAR: integration of instrument and tests*

*G. de Villele*

*J. Pereira do Carmo*

*A. Hélière*

*A. Lefebvre*

*et al.*



## ATLID, ESA Atmospheric LIDAR: integration of instrument and tests

de Villele G 1 , Pereira Do Carmo J 2 , Helière A 2 , Lefebvre A 2 , Barbaro L 1 , Belhadj T 1 ,  
Chassat F 1 , Corselle B 1 , Evin R 1 , Feral M 1 , Levret I 1 , Lingot P 1 , Olivier F 1 , Pelletier S 1 ,  
Pochet J 1 , Schaube A 1 , Varlet F 1 , Vlimant P 1  
1 Airbus Defence And Space, Toulouse, France  
2 European Space Agency - ESTEC., Noordwijk, The Netherlands

### ABSTRACT

The ATmospheric LIDar (Light Detection and Ranging), ATLID, is part of the payload of the Earth Cloud and Aerosol Explorer (EarthCARE) mission, the sixth Earth Explorer Mission of the European Space Agency (ESA) Living Planet Program. After the successful major step of optical and electrical integration, ATLID has started its performance and functional testing in Toulouse Airbus Defence and Space. The emission part of the instrument has been operated with both TxA (Laser transmitter units) delivered from Leonardo team: as major achievement the main performance of both flight lasers have been tested and confirmed with more than 40mJ UV emission @51Hz with operation via instrument control ACDM flight unit (ATLID control and data management). Tests are parallelized with on one side the EFM test (Electrical Flight Model), and on the other side the OFM tests (Optical flight model). The EFM tests aim at validating the functional and electrical architecture via functional testing on each nominal and redundant path with all the flight electronic units and laser sources. The OFM tests aims validating the receiver alignment from telescope input till fiber detectors, the field of view of the three detection channels and their radiometric performance. OFM vibration tests have been performed and have validated design stability against mechanical loads. End of OFM and EFM tests is planned at summer 2018 and will give go ahead for instrument assembly in its final ATLID PFM configuration with laser cooling system integration. After Ambient performance testing, the environmental test campaign immediately start with EMC, mechanical and thermal vacuum testing.

**Keywords:** Lidar, Aerosol, Clouds, UV laser

### 1. INTRODUCTION

The Earth Explorer Core Missions are elements of the European Space Agency Earth Observation Envelope Programme. They are defined as major missions led by ESA to cover primary research objectives set out in the Living Planet Program. EarthCARE (Figure 1)[1], the Earth Clouds Aerosols and Radiation Explorer, has been selected for implementation as the third Earth Explorer Core Mission and is being developed in cooperation with the Japan Aerospace Exploration Agency (JAXA) who provides one of the active instruments. The fundamental objective of EarthCARE is to improve the understanding of the processes involving clouds, aerosols and radiation in the Earth's atmosphere. Clouds and aerosols are currently one of the biggest uncertainties in our understanding of the atmospheric conditions that drive the climate system. A better modelling of the relationship between clouds, aerosols and radiation is therefore amongst the highest priorities in climate research and weather prediction. EarthCARE aims to the determination of cloud and aerosol occurrence, structure and physical properties together with collocated measurements of solar and thermal radiation at a global scale. The mission goals are to retrieve vertical profiles of clouds and aerosols, and the characteristics of their radiative and micro-physical properties, to determine flux gradients within the atmosphere and fluxes at the Earth's surface.

In order to fulfill its objectives, the EarthCARE payload is composed by four instruments, a High Spectral Resolution UV ATmospheric LIDar (ATLID), a 94GHz Cloud Profiling Radar (CPR) with Doppler capability, a Multi-Spectral Imager (MSI) and a Broad-Band Radiometer (BBR). The four instruments will provide, in a synergetic manner, information on cloud and aerosol vertical structure of the atmosphere along the satellite track as well as information about the horizontal structures of clouds and radiant flux from sub-satellite cells.

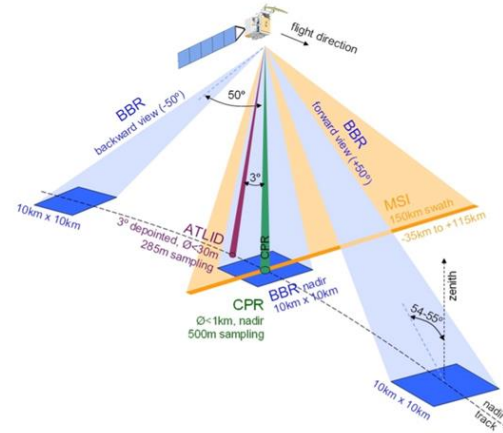


Figure 1 : Artist's view of the EarthCARE satellite in-orbit and its instruments viewing geometry

ATLID is a high spectral Resolution LIDAR in the ultra-violet domain (355nm). The task of ATLID is to provide vertical profiles of optically thin cloud and aerosol layers, as well as the altitude of cloud boundaries. It measures in a direction 3 degrees off nadir, from an altitude of 393 km, with a vertical resolution of about 100 m from ground to an altitude of 20 km and of 500 m from 20 km to 40 km altitude (Figure 2). The instrument transmitter emits short laser pulses with a repetition rate of 51 Hz -corresponding to about 140 m sampling on ground - along the track of the satellite motion, and several shots can be locally averaged to improve the signal to noise ratio. The ATLID receiver collects the backscattered photons with a 62 cm diameter telescope. The UV pulsed energy emitted by the transmitter will be subject to narrow-band particle scattering from atmospheric aerosols, which do not affect the spectrum shape of the incident light, and Rayleigh scattering due to the Brownian motion of atmospheric molecules, which causes broadening of the incident spectrum. ATLID segregates the different backscattering signal contributors by implementing a high spectral resolution filter centered on the emitted wavelength. This way the instrument is able to separate the relative contribution of aerosol (Mie) and molecular (Rayleigh) scattering, which allows the retrieval of the aerosol optical depth. Co-polarised and cross-polarised components of the Mie scattering contribution are also separated and measured on dedicated channels.

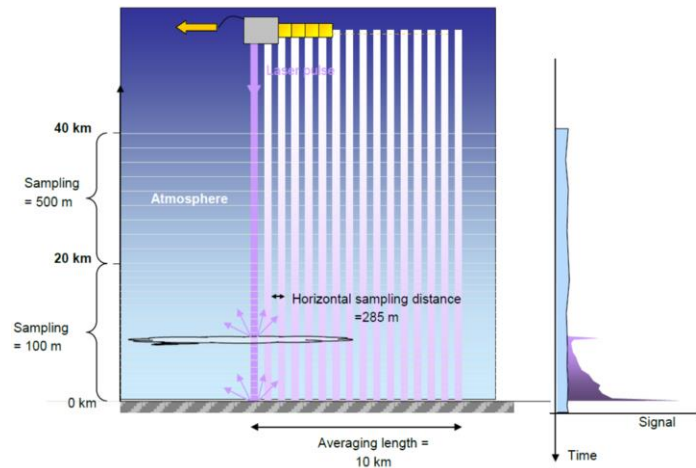


Figure 2 : ATLID resolution and sampling specifications

ATLID, being assembled and tested by Airbus Space and Defense, is designed as a self-standing instrument reducing the mechanical coupling of instrument/platform interfaces and allowing better flexibility in the satellite integration sequence. Following the successful ATLID instrument CDR, completed in 2015, all the PFM sub-systems have now been delivered to Airbus for instrument integration.

The instrument integration is ongoing and the instrument performance and qualification campaign is planned to start late 2018, followed by the instrument delivery to the satellite prime on second quarter of 2019.

## 2. ATLID DEVELOPMENT PLAN: OFM AND EFM

### 2.1 Proto-flight model development

ATLID instrument development is based on proto-flight approach: critical sub-systems such as laser transmitter, beam expander, beam steering mechanism, detector front-end have been subject to specific efforts in terms of early breadboards, electrical models or qualification models to minimize the risks [1][3].

The ATLID instrument development logic and models definition were tailored to allow an efficient development with early validations of the main design drivers to minimize risks. An initial Electrical Engineering Model (EEM) built around representative electronics units, allowed verifying ATLID internal electrical interfaces and software functions, detection chain susceptibility to EMC, and co-alignment control loop function. Then detection Flight Models have been assembled in parallel and used for early verification activities of detection performance.

The instrument is based on a bi-static architecture consisting of two independent main sections, the emitter chain and the receiver chain. The instrument functions are shared between a 'high stability' structure assembly (SSA) (including the telescope, focal plane optics, and the optical emission chain), and a housing structure assembly (HSA) (supporting the electronic units and their radiator, the detection chain and the harness).

The co-alignment loop actuations allow correcting for SSA thermos-elastic deformation expected in orbit. As consequence, the thermo-elastic deformation impact is limited and no instrument structural and thermal model has been tested. The direct integration and testing of a proto-flight model remains a great challenge, in particular due to instrument complexity while there is no direct heritage or recurrent design.

### 2.2 Optical and Electrical parallel program

To anticipate at maximum the instrument verification while the integration is not complete, ATLID PFM verification program is divided into two subprograms: the optical flight model (OFM) and the electrical flight model (EFM) (Figure 3).

The Optical Flight Model (OFM), including the receiver telescope and focal plane assembly installed on the SSA, was used to validate the structural stability of the receiver assembly and for characterization of the optical receiver chain performance. The Electrical Flight Model (EFM), including the HSA with the flight model electronics and harness, was used to establish and verify the electrical coupling between the different units and perform the first part of the instrument functional tests.

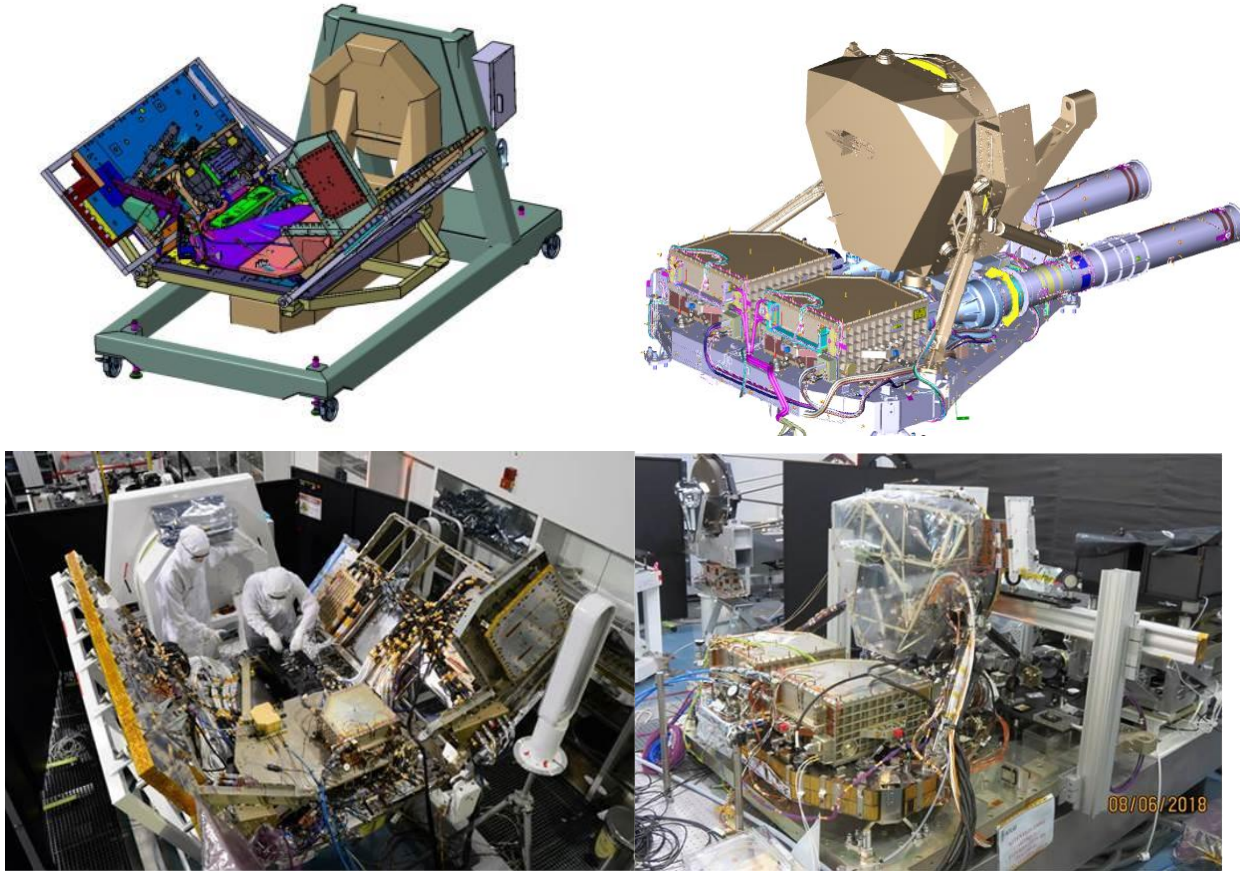


Figure 3 : ATLID EFM model on the left, and ATLID OFM model on the right

Both OFM and EFM programs are parallelized in integration and in testing in Airbus Defence and Space Toulouse cleanrooms.

### 3. OFM MECHANICAL TESTING DESCRIPTION AND RESULTS

#### 3.1 Mechanical test configuration and objectives

The mechanical test consists in applying the spacecraft environments to the systems or subsystems in order to confirm its optical stability as well as its mechanical strength during lifetime. The objective of this OFM mechanical test is to de-risk in advance the most critical parts of ATLID:

- M1/M2 mirrors, as well as the main plate (focal plane assembly support) are composed of Silicon Carbide. This ceramic offers high thermal stability with a great mechanical strength; the development of such brittle structure is inherited from Airbus Defence and Space research and relies on statistic equations.
- Structural adhesive joints reach their maximum limits during sinus environment. The computations and simulations of bonded parts in dynamic environments are key elements derived from modelling and test activities heritage.
- Optical contacting inside the HSRE (High Spectral Resolution Etalon) consists of a molecular adhesion. Its stability under acoustic loads was beforehand checked by random tests and computations. This final test permits to confirm the approach of development chosen.

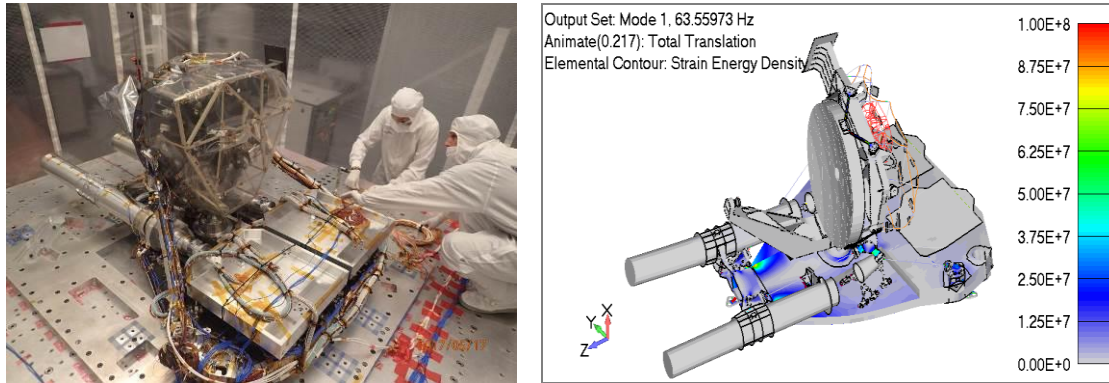


Figure 4: ATLID OFM in Y axis sinus test configuration on shaker at Intespace Toulouse (left) / ATLID OFM FEM Y principal mode @ 63.6 Hz (right)

During the sinus qualification tests, the accelerometers take the control of the shaker. Hence, the choice of these accelerometers and the ability to predict their responses with regards to stress levels on SiC parts, adhesive and optical contacting more particularly remains the most important task of the test (Figure 4).

One criticality for this kind of mechanical test beyond overstress risks is the handling of cleanliness: ISO 5 mobile cleanroom hood was used to ensure controlled environment, also a dedicated protection during acoustic tests.

### 3.2 Mechanical test outcome

The OFM passed with success quasi-static, sinus and acoustic loads applied in the 3 axis configurations, and thus confirm OFM mechanical strength as well as optical stability in Soyuz environments.

More particularly, the superposition of the low level curves, as well as the global / fundamental signals of the qualification runs indicates the structure integrity after Soyuz launch simulation. Moreover, the optical stability was confirmed by the means of theodolite measurements up to better than 100 $\mu$ rad.

In addition, a great correlation between the finite element model and the test results has been observed in term of frequency (<6%). Finally, these results permitted to adjust the finite element model in the frame of the preparation ATLID mechanical test at PFM level.

## 4. OFM RADIOMETRIC TESTING DESCRIPTION AND RESULTS

### 4.1 Optical tests configurations for OFM receiver

ATLID instrument OFM receiver part is composed of the telescope and the Focal Plane Assembly (FPA), where all the receiver optical filtering functions are implemented:

- Large band background rejection and polarization alignment with Entrance Optic Filtering unit (EFO)
- Geometric Receiver Field Of View (RFOV) definition with the Blocking Filtering unit (BF),
- Co-Alignment Sensor (CAS) unit
- High Spectral Receiver Etalon (HSRE) that split the receiver signal onto the three channels of interest for backscattering: Mie Cross-Polarization, Mie Co-Polar, and Rayleigh.
- Fiber Coupling Assembly (FCA) injecting the signals into 3 fibers.

The optical test aims at measuring the OFM characteristics in field of view size, in background rejection, in receiver channel transmission. The 3 channels verification at OFM level does not include flight detectors which are deported on ATLID external radiator via optical fibers.

Due to the reduced RFOV and the high resolution filtering stage, the OGSE (Optical Ground Support Equipment) source and injection performance becomes critical to ensure proper instrument characterization: this includes collimation control taking into account instrument defocus effect of gravity or air to vacuum, the vignetting control in the reduced RFOV, the polarization purity control, the OGSE laser source frequency stability and adjustability, and energy monitoring.

### 4.2 OFM receiver characterization results

The obtained results are in line with ATLID radiometric budget. Spectral scanning transmissions and angular spatial scanning are as expected (Table 1, Figure 5). Moreover, these performance been confirmed after OFM environmental vibration tests.

Table 1 : OFM received characteristics measured on ground

OFM receiver Characteristic	Value measured on ground
RFOV diameter	65 $\mu$ rad
Wide band transmission outside interferometric filter	<0.01%
Mie-Copolar transmission max	54%
Mie-Cross polar transmission max	60%
Rayleigh transmission max	61%

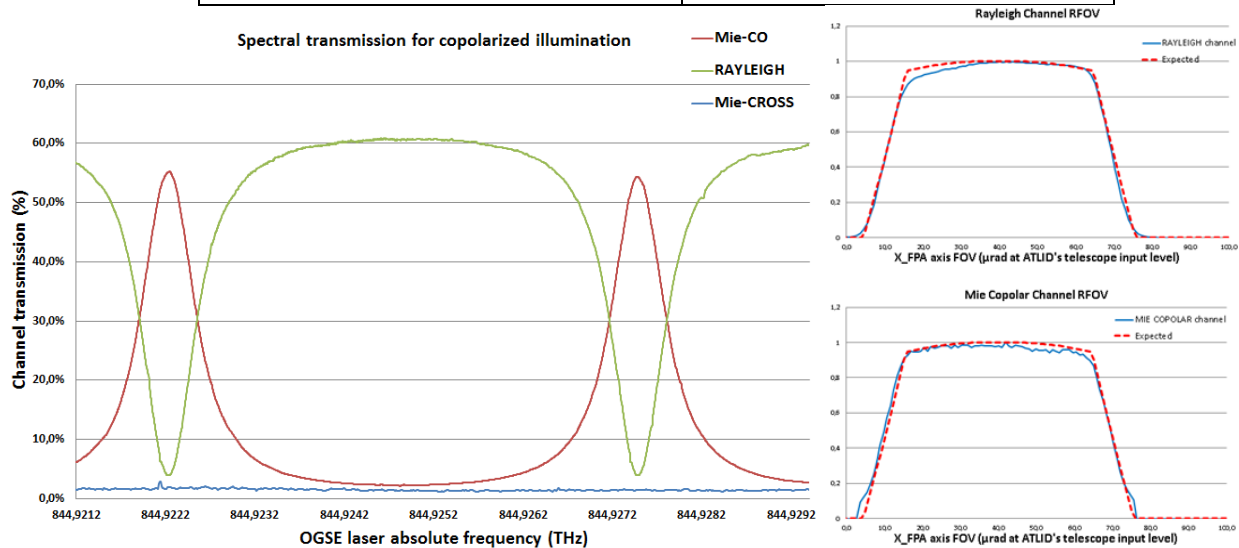


Figure 5 : OFM receiver spectral transmittance scan for copolar illumination (left) and uniformity on angular scan on Rayleigh and Mie Copolar RFOV channels (right)

### 4.3 OFM transmitter path alignment completion

OFM transmitter path is composed of the power laser heads (PLH) and of the External Beam Expander (EBEX) and the long External Baffle tubes (EBaffle) that protect last transmitter UV window from contamination.

PLH and EBEX models have undergone full qualification and acceptance verification respectively at Leonardo and Sodern subcontractor level. Obtained performances are great achievement for ATLID budgets (Table 2). For integration at ATLID instrument level, the transmitter verification aimed at the alignment achievement: transmitters have been aligned with receiver line of sight at better than  $\pm 70 \mu$ rad.

Table 2 : ATLID transmitter path characteristics at instrument exit.

Characteristic	Value at ATLID exit <i>(from PLH output measurement)</i>
Divergence at d4sigma	28 $\mu$ rad
Beam size at d4sigma	60x68mm <sup>2</sup>
Line of Sight compensation range	+/-300 $\mu$ rad on both axis
Wavelength adjustability	+/- 12.5GHz coarse, +/- 0.5GHz fine
Spectral width	< 50 MHz @ FWHM
Wavelength stability	<3 MHz over +/-1 $^{\circ}$ C (orbital)
Energy	41mJ
Pulse duration	28ns

## 5. EFM TESTING DESCRIPTION

### 5.1 EFM detection program completion

The flight instrument detection electronics (IDE) together with the detector fiber assembly (DFA) have been characterized during a dedicated test at equipment level, operated by ACDM EM model (ATLID control and data management). This test was performed in Airbus Defence and Space in vacuum chamber to allow nominal operation of detectors at -30 $^{\circ}$ C as for flight.

Operation tests on IDE validated the detection mode such as LIDAR (nominal echo recording with variable accumulation of profile), and IMAGING for verification of fiber centering on detector. The validation was performed using a dedicated UV source with determined temporal echo profile.

Detection performances have been characterized and comply with ATLID performance needs. (Refer to Table 3)

Table 3 ATLID FM detection chain performance measurement results

Characteristic	ATLID EFM detection measurement
Vertical sampling	100m samples = 22.00Tmc 500m samples = 106.00Tmc WC error 0.02Tmc = 10cm of sample depth
Vertical crosstalk on adjacent samples	4.5% on 500m, 19% on 100m
Computed quantum efficiency MieCoPo/MieCross/Rayleigh	79%/75%/79%
Linearity	<+/-1% from 10e- to the top <+/-2% from 1e- to 10 e-
Dynamic margin on channels wrt predicted worst signal MieCoPo/MieCross/Rayleigh	18%/5%/12%
Noise worst case	2.2 e- rms

### 5.2 EFM functional testing

ATLID instrument is autonomous and requires minimum control by the satellite platform control unit; ATLID onboard software ensures all equipment telecommands and telemetries management, with general monitoring. It creates the data flow, ensures thermal control and co alignment loop control, and also manages the timing synchronization.



As first step of EFM testing, the redundant path has been fully operated and submitted to systematic tests to validate operability and functionality via ATLID Control and Data Management unit (ACDM). Throughout 58 tests procedures, all modes were tested using several thousands of automated checks, including calibration modes and Fault Detection and Isolation (FDIR) triggering.

Laser head was operated at full power with nominal flight operation procedures with a set of parameter adapted for ground usage. Adjustability of PLH internal parameters such as heating currents, nonlinear crystal temperature and pump timings has been demonstrated (Figure 6). The validation of the laser operation with instrument flight hardware is major successful step of functional verification.

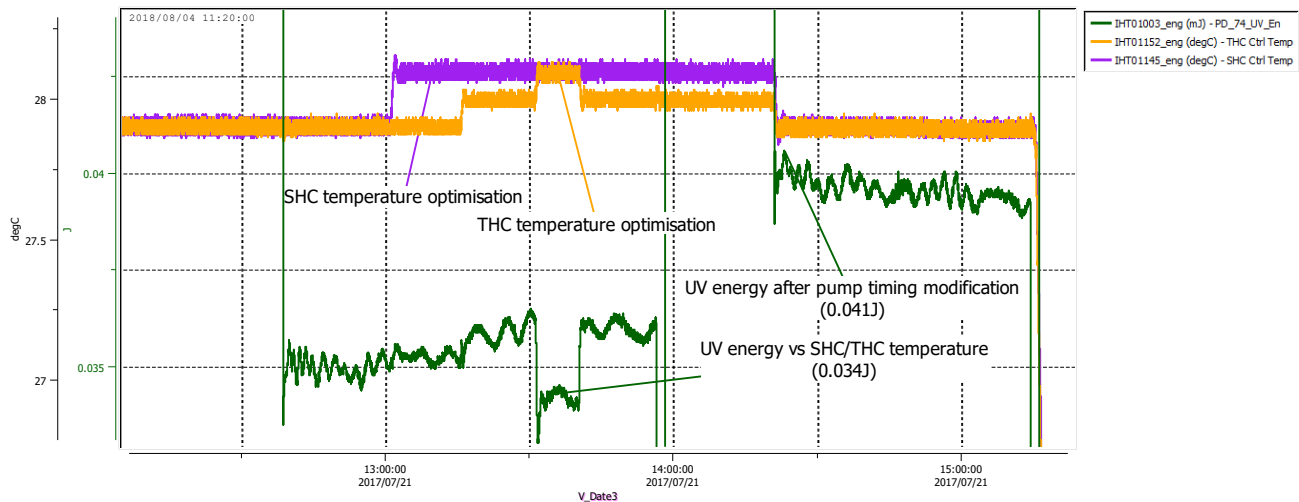


Figure 6 : Example of laser parameter control during first laser switch ON with ACDM unit.

## 6. PFM FINAL ASSEMBLY AND LCS INTEGRATION AND VALIDATION

### 6.1 Assembly and validation of the Laser Cooling System

The Laser Cooling System (LCS) consist in a nominal and redundant network 2x4 diphasic mini Loop Heat Pipes (Figure 7, Figure 11), ensuring 148W extraction from the operating laser. The PLH temperature is thus controlled at 24°C +/-0.5°C within one orbit, while its thermal interface is being mechanically insulated from instrument housing thanks to the flexible piping conducting the heat to an external radiator of 1.05 m<sup>2</sup> placed on the anti-sun side of the Instrument. The design is an innovating one, having the mini-LHPs operated in parallel, and the flexibility to select 1 configuration between 4 in flight (2 main configurations with 6 operated LHPs, and 2 back-up configurations with 5 or 7 LHPs). Design was elaborated by Airbus in Toulouse, while the integration and the test campaign of the LCS have been done by European Heat Pipes (EHP) in EHP premises.

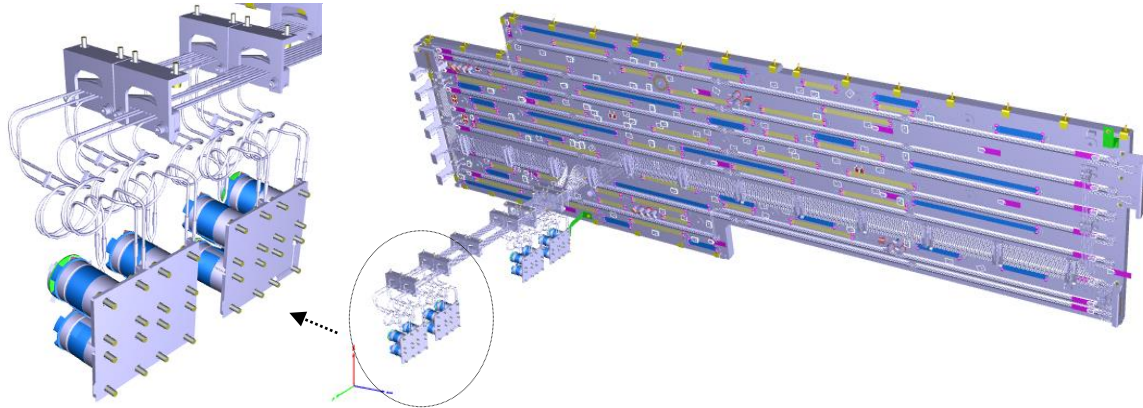


Figure 7 : Evaporators interface to the PLHs and LCS view from its internal side

Testing of LCS thermal performances has been done at LCS level, with the LCS in 2D configuration (evaporators at the same level than the radiator) to reduce the effect of ground gravity, allowing to test the LCS in a representative way, close to flight performances. The test validated the electrical thermal hardware, and also the safe mode of LHP inhibition system, allowing to stop excessive cooling of PLH during non operating phases. Flight performances have been confirmed and 6 loops operation out of 8 has been found optimum considering PLH dissipation evolution since program start. The 2D tests also demonstrated the startup sequence based on heater power distinct from PLH dissipation.

After the completion of the 2D phase, the LCS has been reconfigured to its final 3D shape. Thermal qualification of the 3D LCS was successfully achieved, with vacuum non operative thermal cycles. A dedicated good health test (GHT) was implemented to confirm each LHP ability to startup after boost of power.

## 6.2 ATLID PFM final integration completion and characterization in ambient

The ATLID PFM final integration consists in the mounting of the SSA supporting the OFM inside of the HSA from EFM program; all final flight electrical connection, including also optical fiber will be achieved at this level. Also the LCS will be integrated, with careful handling to avoid any damage especially on the ammonia tubes which are only 2 mm in diameter (Figure 8).

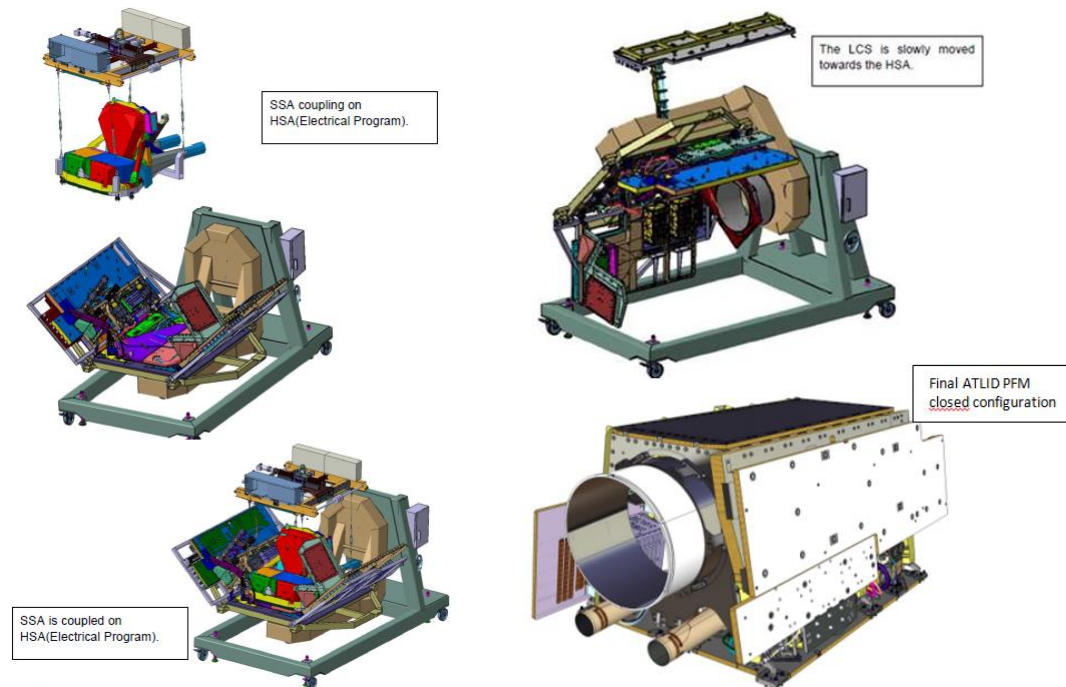


Figure 8 final integrations sequence: SSA coupling in HSA (left), LCS coupling in HSA (top right), final closed configuration (bottom right)

The LCS coupling will be followed by a Good Health Test on each of the 2 buses of the LCS, based on the one elaborated at LCS level, but this time connected to the flight PLH units and with using the flight start-up heaters. At last step, before closing, new instrument functional testing will be performed.

After closing the ATLID PFM instrument tests will start with ambient testing. These are aimed at characterizing the ATLID performance in ambient conditions. Several characteristics verification can be closed at this stage, being independent from environment, other will be degraded vs orbit environment, but will be the first occasion to correlate model and ensure full mastering of end to end performance. Overall the ambient test is a full repetition of the thermal vacuum testing, with using identical OGSE (Figure 9, §7.2)

Ambient testing also includes the electrical testing of the ATLID thermal harness, followed by the validation of the ACDM thermal functions.

Last, the co-alignment control loop will be closed during ambient testing thanks to OGSE returning attenuated emitted signal into the receiver part, at the level of atmospheric backscattering signal, but with adjustment of ACDM timings. A perturbation on the return signal line of sight will test the loop correction and characterize its reaction. It will be end to end validation including the receiver co-alignment sensor (CAS), the Beam Steering Actuator (BSA) in the transmitter, and the software module of the ACDM.

## 7. PFM ENVIRONMENTAL TEST CAMPAIGN OVERVIEW

### 7.1 ATLID PFM vibration test

The finite element model has been affined with the final objective to be delivered to Soyuz launcher once coupled on the satellite for Soyuz input notch instruction.

The PFM test sequence is then similar to the one applied at OFM level refers to §3.1, including a control of optical chain stability, and the associated cleanliness control.

Even if the most critical parts are already tested, refers to §3.1, the PFM test remains the final validation of the whole assembled instrument, and, the confirmation of LCS development assumptions.

Indeed, due to its specific design, refers to Figure 7, the stiffness of its interface has a strong influence on the LCS dynamic behavior. Its junction between 2 majors and independent primary structures, i.e. in one hand on the PLHs of SSA (from OFM), and on the other hand, to the HSA (supporting EFM) increases consistently its mechanical specificity and complexity.

The knowledge of both structure behaviors, already tested on a shaker, OFM & HSA in dynamic environments gives a consistent accuracy and confidence on the FEM prediction.

During the PFM test campaign, the various components of ATLID will be subjected to a range of acceleration varying from 10 g to 120 g, (depending on their location on the structure). In this frame, the 1<sup>st</sup> ATLID mode on infinitely stiff interface is above 60 Hz (i.e. OFM lateral mode Y 61.3 Hz coupled in ATLID structure).

## **7.2 ATLID PFM thermal vacuum test**

The ATLID PFM Thermal Vacuum test will be performed in Centre Spatial de Liège facilities (CSL), in Focal 5 chamber (Figure 9). The Instrument will be placed in the vacuum chamber inside a thermal tent to simulate the thermal space conditions (Figure 10). Vacuum OGSE includes a large collimator of 70cm to cover receiver telescope, a periscope that collect the emitter pulse for monitoring and reinjection in receiver. Outside vacuum chamber, through optical window is a multipurpose OGSE focal plane with monitoring of energy, far field, and with polarization and line of sight control. The OGSE laser source is fiber injected in this focal plane.

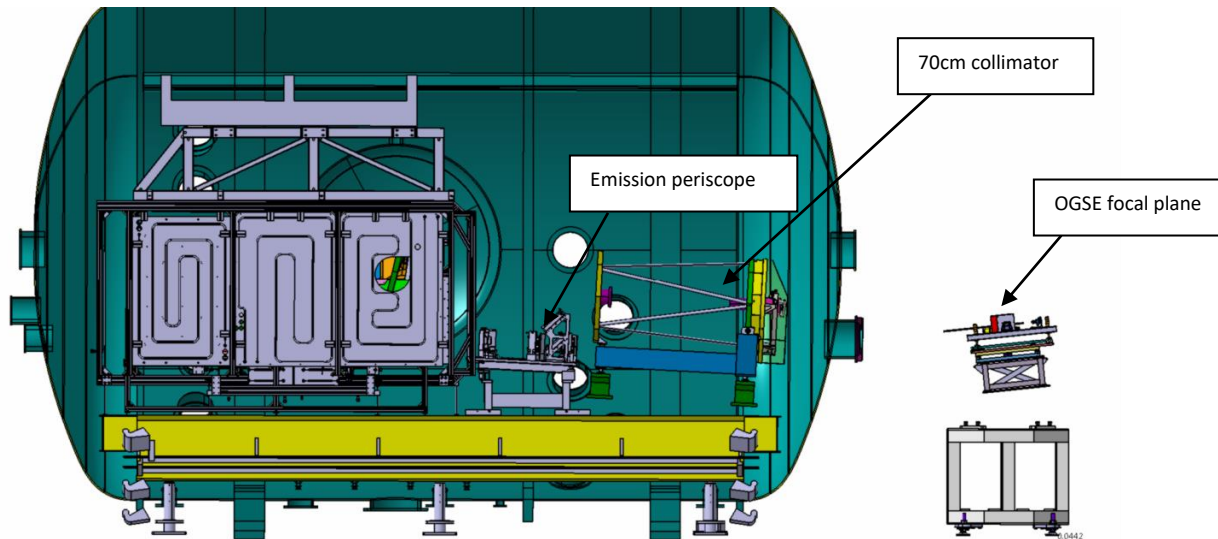


Figure 9 : ATLID TV test set-up, inside Focal 5 chamber

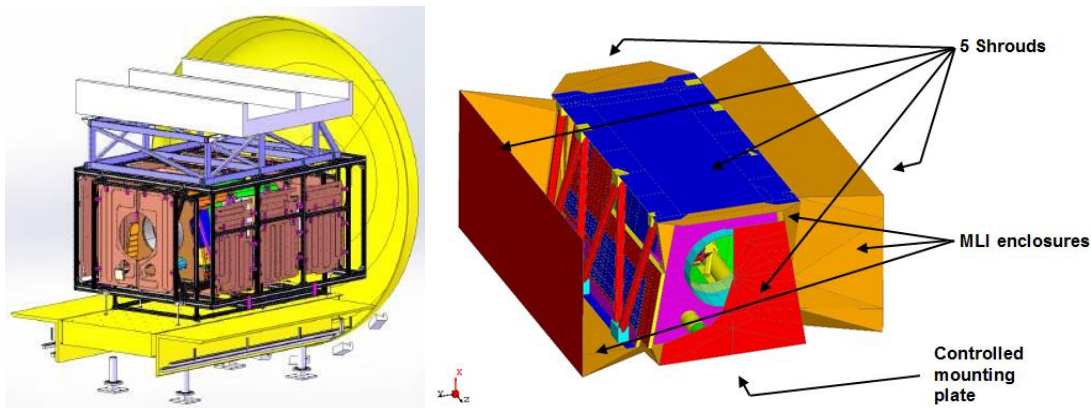


Figure 10 : ATLID in the Thermal Tent

The Test sequence consists of the following activities:

- Instrument Bake-out, with temperature limited at ATLID level to 50°C due to sensible units such as E-BEX.
- NOP phase with representative environment temperatures, including a Thermal Balance for thermal model correlation purpose, and verification of the safe mode thermal hardware and thermal design.
- Operating Phases for the Instrument configurations A and B, including, including a hot and a cold Thermal Balance in operating mode, performances tests in hot and cold conditions, thermal cycling, and orbital cycling with representative environment temperatures.

Due to the orbit definition at 400 km and Mean Local Solar Time 13:45-14:00, the +Y side of ATLID is submitted to variable sun fluxes, while the -Y side of ATLID is not exposed to sun. During the ATLID TV, the operating orbital cycling consists with fluctuations of the +Y shroud in front of the Telescope radiator from -85°C to +15°C typically, while the variations on the -Y side are limited to 20°C in amplitude typically.

The ATLID TV set-up presents some particularities with regards the operations of the PLHs: the performances validation tests will be conducted using an external chiller to extract the PLH dissipation, thanks to a dedicated heat exchanger installed around the LHP evaporators (see Figure 11). This will allow operate the PLH in a known heat extraction reference configuration, rather than in an unusual LCS 3D configuration inducing different thermal performances with gravity. This will be achieved by preventing the LCS to operate during the PLH performance checks, by heating the LCS radiator to 20°C typically.

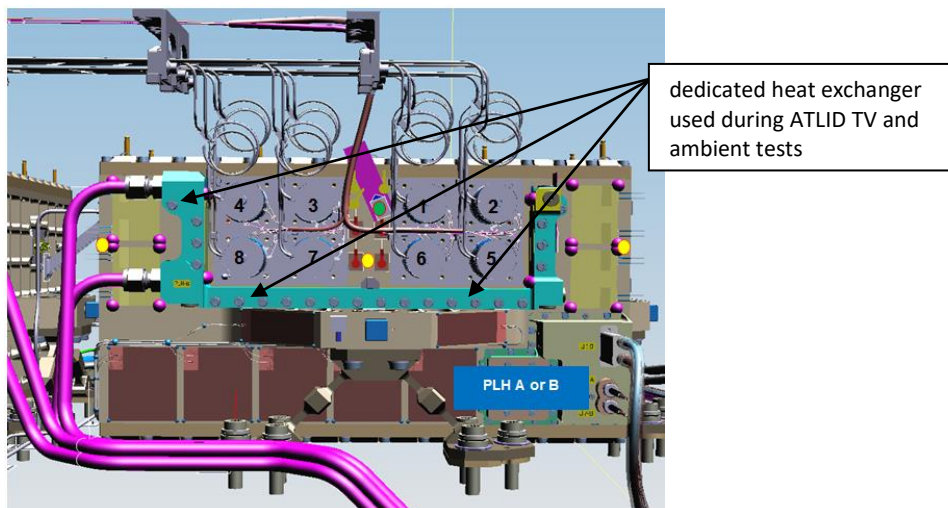


Figure 11 : LCS 8 mini loop evaporators on the PLH and the FSCP heat exchanger system

Since the ATLID Instrument is sensitive to laser induced contamination (LIC) effects, particular precautions shall need to be taken during the ATLID TV campaign. First, all used materials are LIC compatible and will be submitted to bake-out during the ATLID TV preparation, and several cold traps will be installed in the chamber. The emission path, being the most LIC-critical, will also be protected by an extension tube closed by a dedicated OGSE window, attached to the Emission channel baffles. With such design any LIC effect, should it happen, will only impact the OGSE window, and not the flight EBEX window, that is the last and lonely optic being exposed to vacuum in orbit. The transmission will also be continuously monitored during the TV, at several places, and compared to the PLH internal emission energy sensor, which will allow observing and characterizing any transmission losses due to potential LIC effect on OGSEs.

## 8. CONCLUSION

ATLID is now in its last steps of development: the results obtained up to now are very promising for performance, suggesting the fulfillment of EarthCARE mission objectives. The protoflight approach risk has been mitigated with separate optical and electrical program allowing parallelizing the activity. The next months will confirm the final performance of the instrument, in an end to end testing sequence.

The ALADIN LIDAR instrument experience [4][5] is (and will remain) a great advantage for ATLID, allowing to improve design and testing all along the development phase. Today, with the MERLIN LIDAR instrument [6] and thanks to ESA and CNES, Airbus Defence and Space is in charge of 3 LIDAR instruments, gaining maturity and lessons learnt on such difficult and complex instruments.

## REFERENCES

- [1] EarthCARE , <http://www.esa.int/esaLP/LPearthcare.html>
- [2] A. Hélière, L. Le Hors, 2014: Development of ATLID, the EarthCARE UV backscatter LIDAR, ICSO 2014.
- [3] J. Pereira do Carmo, A. Helie, L. Le Hors, Y. Toulemont, A. Lefebvre, 2015: ATLID, ESA Atmospheric LIDAR development status, IRLC 2015.
- [4] ADM-AEOLUS, [https://www.esa.int/Our\\_Activities/Observing\\_the\\_Earth/Aeolus/Introducing\\_Aeolus](https://www.esa.int/Our_Activities/Observing_the_Earth/Aeolus/Introducing_Aeolus)
- [5] Fabre, Frédéric & Culoma, Alain & Moraçais, Didier & Schillinger, Marc & Barthès, Jean-Claude & Endemann, Martin & Durand, Yannig. (2017). ALADIN: the first european lidar in space. 28. 10.1117/12.2307984.
- [6] Alpers, Matthias & Millet, Bruno & Ehret, G & Bousquet, Philippe & Bode, M & Wührer, C. (2017). Merlin: an integrated path differential absorption (IPDA) lidar for global methane remote sensing. 100. 10.1117/12.2296115.